

Integrated omics analysis reveals differences in gut microbiota and gut-host metabolite profiles between obese and lean chickens

Jie Liu,^{*,†} Jie Wang,^{*,†} Yan Zhou,^{*,†} Haixia Han,^{*,†} Wei Liu,^{*,†} Dapeng Li,^{*,†} Fuwei Li,^{*,†}
Dingguo Cao,^{*,†} and Qiuxia Lei^{*,†,1}

**Poultry Institute, Shandong Academy of Agricultural Sciences, 250100, Ji'nan, China; and [†]Poultry Breeding Engineering Technology Center of Shandong Province, 250100, Ji'nan, China*

ABSTRACT Abdominal fat is the major adipose tissue in chickens. In chicken, the deposition of abdominal fat affects meat yield and quality. Previous reports suggest that gut microbiota composition and function are associated with lipid metabolism. In this study, we used comparative metagenomics and metabolomics analysis to determine the gut microbiota and gut-host metabolite profiles in Shouguang (**SG**; a Chinese chicken breed with low-fat deposition) and Luqin (**LQ**; a fatty-type chicken breed with a fast growth rate) chickens. The results showed that LQ chickens had higher body weight, eviscerated yield, abdominal fat yield, abdominal fat ratio, and triglyceride (**TG**) content in the breast muscle than SG chickens. Untargeted metabolomics analyses showed a total of 11 liver metabolites, 19 plasma metabolites, and 30 cecal metabolites differentially enriched in LQ and SG chickens based on variable importance in the projection (**VIP**) ≥ 1 and $P \leq 0.05$. These metabolites are involved in lipid and amino acid

metabolism. The relative abundance of bacteria in the microbiota differed significantly between the 2 chicken breeds. The functional prediction of microbiota abundant in LQ chickens was starch and lactose degradation. *Erysipelatoclostridium* was abundant in LQ chickens and significantly positively correlated to palmitoyl ethanolamide (**PEA**), a key regulator of lipid metabolism. Our findings revealed differences in liver and plasma metabolites between chicken breeds with different adipose deposition capacities. Long-chain acylcarnitines might be important markers of adipose deposition differences in chickens. The cecum's microbial communities and metabolome profiles significantly differed between LQ and SG chickens. However, the relationship between cecal microbiota and their metabolites and liver and plasma metabolites is not thoroughly understood. Future research will focus on relating tissue metabolite changes to intestinal microbiota and their effects on body fat deposition.

Key words: microbiome, metabolome, chicken, fat deposition

2022 Poultry Science 101:102165

<https://doi.org/10.1016/j.psj.2022.102165>

INTRODUCTION

Chickens are one of the most important agricultural animals (Burt, 2007). The rise in the production and consumption of chicken meat and related products is responsible for forming by-products. Among these, abdominal fat, the primary adipose tissue in chickens, is considered waste and discarded, creating an environmental problem (Peña-Saldarriaga et al., 2020). Moreover, excessive fat deposition decrease feed efficiency and cause consumer rejection (Tumová and Teimouri,

2010). Chickens can be used as a biomedical model to study human metabolic disorders, such as insulin resistance, diabetes, obesity, and metabolic syndrome (Stern, 2005; Braun and Sweazea, 2008). Therefore, understanding the molecular mechanisms of abdominal adipose tissue deposition can provide insight into biomedical research and benefit poultry production.

The biological mechanisms that regulate the synthesis and degradation of lipids and lipid transport in liver and plasma play a role in adipose tissue deposition (Baéza et al., 2015). The intestine is the major site of food transformation and metabolism, and the gut microbiota is important for nutrient and energy metabolism (Turnbaugh et al., 2006). Increased studies have demonstrated that intestinal microbes can affect host lipid metabolism through multiple direct and indirect biological mechanisms. Conventionally raised (**CONV-R**) and germ-free mice studies showed that the serum metabolome of

© 2022 The Authors. Published by Elsevier Inc. on behalf of Poultry Science Association Inc. This is an open access article under the CC BY-NC-ND license (<http://creativecommons.org/licenses/by-nc-nd/4.0/>).

Received May 6, 2022.

Accepted August 19, 2022.

¹Corresponding author: jqs_saas@163.com

CONV-R mice was characterized by increased energy metabolites levels (Velagapudi et al., 2010). Moreover, the microbiota modified several lipid species in the serum, adipose tissue, and liver, with its greatest effect on TG and phosphatidylcholine species. The trimethylamine N-oxide (TMAO) levels have been implicated in atherosclerosis in mice and humans. TMAO is derived secondarily through hepatic oxidation of trimethylamine produced through gut microbe-mediated metabolism of dietary choline and L-carnitine (Koeth et al., 2013). Some facultative and anaerobic bacteria in the large intestine produce secondary bile acids from the pool of bile salts secreted into the intestine. A small fraction of these bacterially derived bile acids is absorbed into the bloodstream and can modulate hepatic and/or systemic lipid and glucose metabolism through nuclear or G protein-coupled receptors (Ghazalpour et al., 2016). Therefore, both host and intestinal microbes regulate lipid-related phenotypes.

A systematic study of metabolites in plasma and liver and gut microbiota and their metabolites can be used to understand the molecular mechanisms of adipose tissue deposition. This study investigated the composition of metabolites in liver, plasma, and cecum using liquid chromatography with mass spectrometry (LC-MS)-based metabolomics approach and explored the differences in the cecal microbiome using metagenomic sequencing between lean and fat chicken breeds.

MATERIALS AND METHODS

Ethical Approval

All animal experiments were conducted in accordance with the Guidelines for Experimental Animals, established by the Ministry of Science and Technology (Beijing,

China). Animal experiments were approved by the Science Research Department of the Shandong Academy of Agricultural Sciences (SAAS) (Ji'nan, China). Ethical approval for animal survival was given by the animal ethics committee of SAAS (No. SAAS-2019-029).

Animals

We obtained Shouguang (SG) and Luqin (LQ) chicken breeds reared in the same environment from the Poultry Institute, Shandong Agriculture Academy Science. A total of 120 female birds (60 from each breed) were used. The cages in the experimental station were arranged in a semi-ladder coop. Chickens were fed ad libitum. Management of the feeding schedule and basal diets (Table 1) were based on the Feeding Standard for Chickens established by the Ministry of Agriculture. At 160 days of age, we obtained 5 mL blood samples from the wing vein of 16 chickens (8 from each breed). The plasma was harvested following centrifugation at $1,000 \times g$ for 10 min. The plasma samples were frozen in liquid nitrogen and stored at -80°C . The 16 chickens were euthanized by stunning and exsanguination. Liver tissue samples were harvested, frozen in liquid nitrogen, and stored at -80°C . The cecum contents were collected aseptically, snap frozen, and stored at -80°C . The carcasses were manually eviscerated and dissected, and abdominal fat weight was estimated. The percentage of abdominal fat weight was expressed as a ratio of eviscerated yield. The breast muscle's TG content was determined using kits obtained from Nanjing Jiancheng Bioengineering Institute (Nanjing, China). We homogenized 0.1 g of muscle sample in 0.9% saline and centrifuged the samples at $2,500 \times g$ for 15 min at 4°C . The

Table 1. Composition and nutrient levels of the basal diet.

Items	Content		
	1 to 28 day of age	29 to 56 day of age	57 to 160 day of age
Ingredients (%)			
Corn	62.30	66.01	69.80
Soybean meal	27.50	23.00	12.50
Corn gluten meal	4.50	4.00	5.00
Wheat bran	1.80	2.17	6.88
Soybean oil	0.30	1.50	2.80
Limestone	1.00	0.80	0.75
CaHPO ₄	1.78	1.70	1.45
NaCl	0.320	0.320	0.320
Premix ¹	0.50	0.50	0.50
Total	100.00	100.00	100.00
Nutrient levels ²			
CP	21.06	19.09	16.05
ME(MJ/kg)	12.18	12.59	13.00
Met+Cys	0.85	0.72	0.65
Thr	0.76	0.74	0.65
Lys	1.05	0.98	0.85
Ca	1.01	0.91	0.80
P	0.68	0.65	0.60

¹The premix provided the following per kg of diets: VA 6,000 IU, VD₃ 1,000 IU, VE 15 IU, VK₃ 0.5 mg, VB₁ 2 mg, VB₂ 4 mg, D-pantothenic acid 10 mg, nicotinic acid 35 mg, VB₆ 3.5 mg, VB₁₂ 0.01mg, biotin 0.18 mg, folic acid 0.55mg, Cu (as copper sulfate) 8 mg, Fe (as ferrous sulfate) 90 mg, Mn (as manganese sulfate) 90 mg, Zn (as zinc sulfate) 650 mg, Se (as sodium selenite) 0.20 mg.

²The nutrient levels were measured values.

supernatant was used to determine TG content. The data on host carcass traits and TG content are presented as mean \pm standard deviation (**SD**). Significant differences between the breeds were evaluated using Student's *t* test (SPSS 22, IBM, Armonk, NY).

Metabolite Extraction

Metabolites were extracted as previously reported (Xiang et al., 2021). The collected samples were thawed on ice. The metabolites were extracted from 20 μ L of each sample using 120 μ L of precooled 50% methanol buffer. The metabolites mixture was vortexed for 1 min, incubated at room temperature for 10 min, and stored overnight at -20°C . The mixture was centrifuged at $4,000 \times g$ for 20 min. The resulting supernatant was transferred into 96-well plates, and stored at -80°C prior to LC-MS analysis. Pooled quality control (**QC**) samples were prepared by combining 10 μ L of each extraction mixture.

LC-MS Analysis

All samples were analyzed using a TripleTOF 5600 Plus high-resolution tandem mass spectrometer (SCIEX, Warrington, UK) in positive and negative ion modes (Cao et al., 2020). An ultraperformance liquid chromatography (**UPLC**) system (SCIEX, UK) was used for chromatographic separation. An ACQUITY UPLC T3 column (100 mm \times 2.1 mm, 1.8 μ m, Waters, UK) was used for the reversed-phase separation. The mobile phase consisted of solvents A (0.1% formic acid in water) and B (0.1% formic acid in acetonitrile). The gradient elution conditions performed at 0.4 mL/min were the following, 5% solvent B for 0 to 0.5 min; 5% to 100% solvent B for 0.5 to 7 min; 100% solvent B for 7 to 8 min; 100 to 5% solvent B for 8 to 8.1 min; and 5% solvent B for 8.1 to 10 min. The column temperature was maintained at 35°C .

The TripleTOF 5600 Plus system was used to detect the eluted metabolites. The curtain gas pressure was 30 PSI, and the ion source gas 1 and gas 2 pressure was 60 PSI. The interface heater temperature was 650°C . The ion spray floating voltage was 5 kV for the positive-ion mode and -4.5 kV for the negative-ion mode. The MS data were acquired in the IDA mode. The TOF mass range was 60 to 1,200 Da. Survey scans were acquired every 150 ms. As many as 12 product ion scans were collected when the threshold of 100 counts/s exceeded with a 1+ charge state. The total cycle time was fixed at 0.56 s. Four-time bins were added for each scan at a pulse frequency of 11 kHz by monitoring the 40-GHz multichannel TDC detector with 4-anode/channel detection. Dynamic exclusion was set for 4 s. During the acquisition period, the mass accuracy was calibrated every 16 samples. Furthermore, a QC sample was analyzed every 8 samples to assess the stability of the LC-MS.

Metabolomics Data Processing

The LC-MS data preprocessing was performed as previously described (Pu et al., 2021). Briefly, raw data files were converted into mzXML format and processed using the XCMS, CAMERA, and metaX toolbox included in the R software (Smith et al., 2006; Kuhl et al., 2012; Wen et al., 2017). Each ion was identified by retention time and *m/z*. Each peak intensity was recorded, and a three-dimensional matrix containing arbitrarily assigned peak indices (retention time–*m/z* pairs), sample names (observations), and ion intensity information (variables) was generated. Subsequently, the information was matched to in-house and public databases. The open-access databases KEGG (<https://www.kegg.jp/>) and HMDB (<http://www.hmdb.ca/>) were used to annotate the metabolites by matching the exact molecular mass data (*m/z*) within a threshold of 10 ppm. The peak intensity data was preprocessed using metaX. Features detected in $<50\%$ of QC samples or 80% of test samples were removed, and values for missing peaks were extrapolated with the *k*-nearest neighbor algorithm to further improve the data quality. PCA was performed to identify outliers and batch effects using the preprocessed dataset. QC-based robust LOESS signal correction was fitted to the QC data with respect to the order of injection to minimize signal intensity drift over time. The relative standard deviations of the metabolic features were calculated across all QC samples, and those with standard deviations $>30\%$ were removed.

The group datasets were normalized prior to analyses. Data normalization was performed using the probabilistic quotient normalization algorithm (Dieterle et al., 2006). QC-robust spline batch correction was performed using QC samples. The *P*-value obtained from Student's *t* test was used to identify different metabolites. We conducted supervised partial least-squares discriminant analysis (**PLS-DA**) using metaX to variables that discriminant profiling statistical method to identify more specific differences between the groups. The VIP cut-off value of 1.0 was set to select important features.

Cecal Metagenomics Analysis

The microbiome DNA was extracted from cecal samples using the E.Z.N.A. Stool DNA Kit (D4015-02, Omega, Inc., Norcross, Georgia), and the genomic DNA was used for the library construction. Blunt-end DNA fragments were generated using a combination of fill-in reactions and exonuclease activity, and size selection was performed with sample purification beads. An A-base was added to the blunt ends of each strand, preparing them for ligation to the indexed adapters. Each adapter contained a T-base overhang for ligating the adapter to the A-tailed fragmented DNA. These adapters fully complement sequencing primer hybridization sites for single, paired-end, and indexed reads. Single- or dual-index adapters were ligated to the fragments, and PCR amplified the ligated products. PCR conditions were initial denaturation at 95°C for 3 min, eight cycles

of denaturation at 98°C for 15 s, annealing at 60°C for 15 s, and extension at 72°C for 30 s, and a final extension at 72°C for 5 min. The raw sequence data were deposited in the Genome Sequence Archive (Genomics, Proteomics & Bioinformatics 2021) in the National Genomics Data Center (Nucleic Acids Res 2022), China National Center for Bioinformation / Beijing Institute of Genomics, Chinese Academy of Sciences (GSA: CRA006699) that are publicly accessible at <https://ngdc.cncb.ac.cn/gsa>.

Raw sequencing reads were processed to obtain valid reads for further analysis. First, sequencing adapters were removed from sequencing reads using cutadapt v1.9 (Kechin et al., 2017). Second, low-quality reads were trimmed by fqtrim v0.94 using a sliding-window algorithm. Third, reads were aligned to the host genome using bowtie2 v2.2.0 (Langmead and Salzberg, 2012; Langmead et al., 2019) to remove host contamination. Once quality-filtered reads were obtained, they were de novo assembled to construct the metagenome for each sample by IDBA-UD v1.1.1 (Peng et al., 2012). All metagenomic contigs coding regions were predicted using MetaGeneMark v3.26 (Zhu et al., 2010). Sequences of coding regions were clustered using CD-HIT v4.6.1 (Li and Godzik, 2006) to obtain unigenes. Unigene abundance for a certain sample was estimated by TPM based on the number of aligned reads by bowtie2 v2.2.0. The lowest common ancestor taxonomy of unigenes was obtained by aligning them against the NCBI NR database by DIAMOND v 0.9.14. Similarly, the functional annotation of unigenes was obtained. Based on the taxonomic and functional annotation of unigenes, along with the abundance profile of unigenes, differential analysis was performed at each taxonomic, functional, or gene-wise level by the Mann-Whitney U test.

RESULTS

Carcass Traits and TG Content of Breast Muscle

The carcass traits of LQ and SG chickens were compared at 160 d of age (Table 2). LQ chickens exhibited higher body weight, eviscerated yield, abdominal fat yield, and abdominal fat ratio than SG chickens ($P < 0.01$). Compared to SG chickens, LQ chickens had a higher TG content in breast muscle ($P < 0.01$).

Table 2. Differences in carcass traits and muscle TG content between LQ and SG chickens.

Variable	LQ chickens	SG chickens	<i>P</i> value
Body weight (g)	2,340.00 ± 42.62	2,141.25 ± 140.34	0.005
Eviscerated yield (g)	1,220.38 ± 41.31	1,085.50 ± 111.73	0.011
Abdominal fat yield (g)	155.75 ± 35.97	67.50 ± 23.74	0.000
Abdominal fat ratio (%)	11.29 ± 2.37	5.77 ± 1.75	0.000
TG content (mg/g)	7.59 ± 1.80	2.37 ± 0.76	0.000

Values are presented as the mean ± SD; n = 8 per group.

Abbreviations: LQ, Luqin chicken; SG, Shouguang chicken; TG, triglyceride.

Metabolic Differences Between LQ and SG Chickens

PLS-DA model revealed a clear separation of metabolites from SG and LQ chickens (Figure 1). In liver, the metabolites were pyridines and derivatives, naphthalenes, quinolines and derivatives, macrolides and analogs, fatty acyls, glycerophospholipids, carboxylic acids and derivatives, and sterol lipids. These metabolites are involved in histidine, tryptophan, purine, and beta-alanine metabolism and fatty acid degradation (Figure 2A). In LQ chickens, the relative levels of 4-pyridoxic acid, 2,7-dihydroxynaphthalene, imiquimod, dehydrocarpaine II, acylcarnitine 24:6, lysophosphatidylethanolamine (lysoPE) 20:5, acylcarnitine 26:5 were significantly higher than in SG chickens (Table 3).

The plasma metabolites included fatty acyls, phenols, benzene and substituted derivatives, organic sulfuric acids and derivatives, indoles and derivatives, peptidomimetics, flavonoids, imidazopyrimidines, and quinolines and derivatives. These metabolites participate in vitamin B₆, glutathione, and glycerophospholipid metabolism (Figure 2B). In LQ chickens, the relative levels of fatty acyls were significantly higher than in SG chickens, including acylcarnitine 16:1, palmitoylcarnitine, oleoyl-L-carnitine, stearoyl-L-carnitine, and acylcarnitine 20:1 (Table 4).

The cecum metabolites comprised glycerophospholipids, fatty acyls, carboximide acids and derivatives, sterol lipids, phenanthrenes and derivatives, and glycerolipids. These metabolites participate in glycerophospholipid metabolism and glycosylphosphatidylinositol (GPI)-anchor biosynthesis (Figure 2C). In LQ chickens, the relative levels of mesaconic acid, lysophosphatidylglycerol (lysoPG) 15:0, lysoPG 16:1, phosphatidylethanol (PE) (16:0/16:0), 4,4'-bis(dimethylamino) benzophenone, palmitoyl ethanolamide, and alpha-solanine were significantly higher than in SG chickens. However, the relative levels of 10 lysophosphatidylcholine (lysoPC) (PC 14:0, PC 16:0, PC 16:1, PC 18:3, PC 20:3, PC 20:4, PC 20:5, PC 22:4, PC 22:5, and PC 22:6) and 4 lysoPE (PE16:1, PE18:2, PE20:4, and PE22:6) were significantly lower in LQ chickens compared to SG chickens (Table 5).

Differences in the Cecal Microbiome Between LQ and SG Chickens

To further assess whether differences in cecal microbiota were the causal factor for the differences in cecum content metabolomes between LQ and SG chickens, a metagenomic sequencing analysis of the microbial communities in the cecum of the 2 breeds was performed. A total of 615,371,530 bp clean reads were obtained after quality control. A total of 2.3 million contigs with an average size of 1,085 and an average N50 length of 1,151 bp were produced after subsequent assembly. The differences in bacterial diversity between LQ and SG

Table 3. Differential metabolites in liver between LQ and SG chickens.

Metabolites	RT	FC(LQ/SG)	P-value	VIP	Class	Regulated
4-Pyridoxic acid	2.36	3.25	0.010	2.65	Pyridines and derivatives	up
2,7-Dihydroxynaphthalene	2.74	2.23	0.007	2.16	Naphthalenes	up
Imiquimod	2.91	10.54	0.002	3.98	Quinolines and derivatives	up
Dehydrocarpaine II	8.54	2.59	0.046	1.89	Macrolides and analogues	up
Acylcarnitine 24:6	2.99	2.81	0.046	2.42	Fatty Acyls	up
LysoPE 20:5	4.21	2.05	0.006	2.51	Glycerophospholipids	up
Acylcarnitine 26:5	3.89	2.89	0.019	2.81	Fatty Acyls	up
L-Glutathione, reduced	2.30	0.48	0.035	1.76	Carboxylic acids and derivatives	down
Acylcarnitine 22:5	3.93	0.41	0.002	2.65	Fatty Acyls	down
Cinobufagin	2.76	0.48	0.025	2.00	Sterol Lipids	down
Acylcarnitine 23:5	4.25	0.46	0.005	2.45	Fatty Acyls	down

Abbreviations: FC, fold change; LQ, Luqin chicken; RT, retention time; SG, Shouguang chicken; VIP, variable important for the projection.

chickens were evaluated using diversity and richness estimators (Table S4). Community diversity indexes (Simpson and Shannon) of cecal microbiota were higher in LQ than in SG chickens ($P < 0.05$, Table S5). There were no differences in richness estimators (observed species and Chao1) in the cecal microbiota between the breeds.

Figure 3A shows that Bacteroidetes, Firmicutes, and Proteobacteria were the most predominant phyla in each group. More than 45% of the sequences could be assigned to these phyla in the 2 breeds. At the genus level, the top 10 bacteria in both groups accounted for 45% of the total reads (Figure 3B). The dominant Bacteroides accounted for 20% of the total genera. The genera relative abundance in the 2 breeds is shown in Figure 4A. The results showed that Blautia, Prevotellaceae, Erysipelatoclostridium, Merdibacter, Podoviridae, Acholeplasma, and Anaeroplasmata were significantly upregulated in LQ chickens ($P < 0.05$) and Burkholderiales, Criibacterium, and Pseudobacteroides were significantly downregulated ($P < 0.05$). At the species level (Figure 4B), Clostridiales CHKCI006, Erysipelatoclostridium, Drancourtella, Erysipelatoclostridium ramosum, Muribaculaceae isolate 036 (Harlan), and Clostridium saccharogumia were significantly upregulated in LQ chickens ($P < 0.05$), while Blautia sp. OF03-

13, Pseudobacteroides cellulosolvans, Azospirillum halopraeferens, and Variovorax sp. HW608 were significantly downregulated ($P < 0.05$).

Potential Function of the Cecal Microbiota

The potential function of bacterial communities in LQ and SG chickens was predicted using functional metagenome annotation with the CAZy database. Eighteen CAZy subsystems showed significant differences in their relative abundance between LQ and SG chickens (Figure 5). The LQ chickens had significant enrichments for the subsystems related to starch and lactose degradation, for example, Glycoside Hydrolase Family 86 (GH86), Glycoside Hydrolases Family 13_28 (GH13_28), Glycoside Hydrolases Family 5_44 (GH5_44), Carbohydrate-Binding Module Family 25 (CBM25), and Carbohydrate-Binding Module Family 40 (CBM40).

Correlation Between Microbial Communities and Their Metabolites

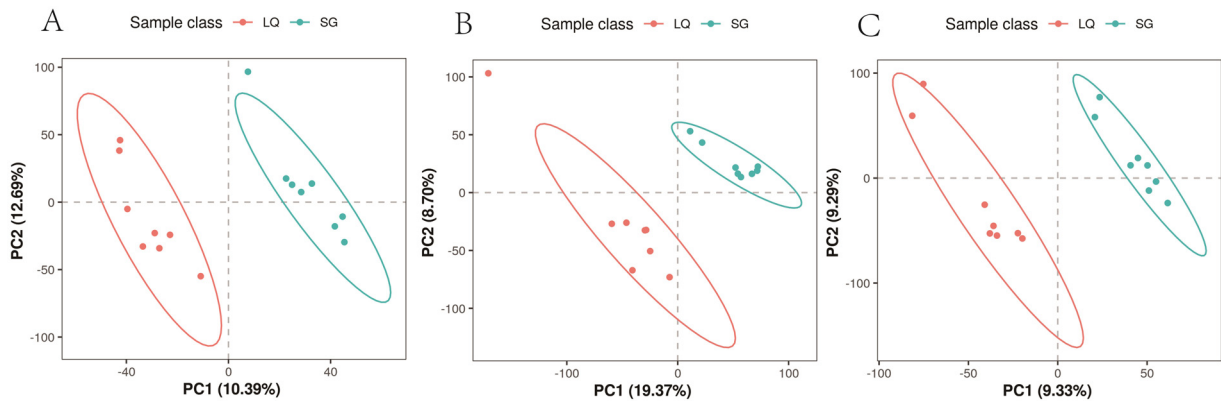
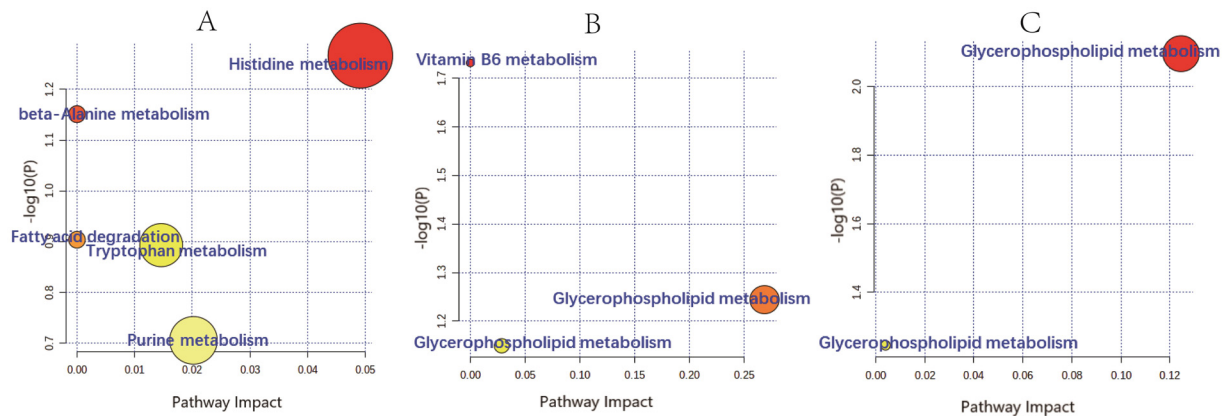
Pearson's correlation analysis of metabolites and 10 genera (Figure 6A) or 10 species (Figure 6B) of microbes showed significant differences between LQ and SG

Table 4. Detection of different metabolites in plasma

Metabolites	RT	FC(LQ/SG)	P-value	VIP	Class	regulated
Acylcarnitine 16:1	3.943	3.04	0.017	3.301	Fatty Acyls	up
Palmitoylcarnitine	4.160	2.41	0.036	2.933	Fatty Acyls	up
Oleoyl-L-carnitine	4.250	3.23	0.025	3.470	Fatty Acyls	up
Stearoyl-L-carnitine	4.569	2.14	0.036	2.826	Fatty Acyls	up
Acylcarnitine 20:1	4.657	2.13	0.043	2.788	Fatty Acyls	up
p-Cresol	3.212	0.45	0.002	3.299	Phenols	down
2,6-Dihydroxybenzoic acid	3.119	0.46	0.001	3.158	Benzene and substituted derivatives	down
p-Cresol sulfate	3.209	0.44	0.003	3.351	Organic sulfuric acids and derivatives	down
1H-Indole-3-propanoic acid	3.518	0.50	0.005	2.949	Indoles and derivatives	down
3-ethylphenyl Sulfate	3.593	0.41	0.021	3.627	Organic sulfuric acids and derivatives	down
Indoxyl sulfate	2.830	0.35	0.001	3.769	Organic sulfuric acids and derivatives	down
L-Anserine	0.908	0.32	0.007	3.345	Peptidomimetics	down
Baicalin	3.007	0.43	0.007	3.041	Flavonoids	down
Apigenin-6-C-glucoside-7-O-glucoside	2.752	0.43	1.13E-05	3.596	Flavonoids	down
Hypoxanthine	1.587	0.28	0.004	4.532	Imidazopyrimidines	down
5-Hydroxyindole-3-acetic acid	2.510	0.43	0.018	2.718	Indoles and derivatives	down
Ethoxyquin	4.135	0.49	0.018	2.784	Quinolines and derivatives	down
Acylcarnitine 5:0	2.749	0.49	0.001	3.102	Fatty Acyls	down
3-Methylglutaryl carnitine	2.613	0.41	0.011	3.489	Fatty Acyls	down

Table 5. Detection of different metabolites in caecum.

Metabolites	RT	FC	P-value	VIP	Class	regulated
Mesaconic acid	1.256	3.42	0.015	3.490	Fatty Acyls	up
LysoPG 15:0	4.631	2.52	0.004	2.965	Glycerophospholipids	up
LysoPG 16:1	4.943	2.51	0.012	2.921	Glycerophospholipids	up
PE(16:0)	4.259	2.40	0.020	2.516	Glycerophospholipids	up
4,4'-Bis(dimethylamino)benzophenone	4.674	9.00	0.042	3.141	-	up
Palmitoyl ethanolamide	6.593	2.03	0.032	2.194	Carboximide acids and derivatives	up
alpha-Solanine	3.014	2.46	0.043	2.198	Sterol Lipids	up
LysoPE 16:1	4.532	0.49	0.038	2.277	Glycerophospholipids	down
LysoPS 18:2	6.025	0.38	0.016	2.635	Glycerophospholipids	down
LysoPE 22:6	4.695	0.41	0.048	2.184	Glycerophospholipids	down
LysoPC 18:3	4.399	0.40	0.022	2.535	Glycerophospholipids	down
LysoPC 20:3	5.065	0.27	0.011	3.055	Glycerophospholipids	down
LysoPC 22:4	5.333	0.49	0.032	2.336	Glycerophospholipids	down
TG 66:21;	4.676	0.12	0.027	3.870	Glycerolipids	down
Val-Gly	0.932	0.44	0.019	2.558	Carboxylic acids and derivatives	down
cis-Nerolidol	5.182	0.42	0.000	2.896	-	down
Oxycodone	2.638	0.47	0.002	2.963	Phenanthrenes and derivatives	down
Acylcarnitine 16:1	3.973	0.47	0.048	2.145	Fatty Acyls	down
LysoPC 14:0	4.372	0.36	0.031	2.488	Glycerophospholipids	down
LysoPE 18:2	4.758	0.46	0.014	2.560	Glycerophospholipids	down
LysoPC 16:1	4.580	0.38	0.007	2.845	Glycerophospholipids	down
LysoPC 16:0	4.930	0.47	0.016	2.437	Glycerophospholipids	down
LysoPE 20:4	4.751	0.38	0.011	2.742	Glycerophospholipids	down
Plasmenyl-PC 17:0	4.920	0.46	0.007	2.602	Glycerophospholipids	down
Plasmenyl-PC 18:0	5.337	0.48	0.024	2.347	Glycerophospholipids	down
LysoPC 20:5	4.352	0.31	0.050	2.511	Glycerophospholipids	down
LysoPC 20:4	4.736	0.29	0.023	2.881	Glycerophospholipids	down
1-Oleoyl-sn-glycero-3-phosphocholine	5.343	0.50	0.017	2.219	Glycerophospholipids	down
LysoPC 22:6	4.740	0.22	0.001	3.867	Glycerophospholipids	down
LysoPC 22:5	5.05	0.38	0.027	2.595	Glycerophospholipids	down

**Figure 1.** Partial least-squares-discriminant analysis (PLS-DA) for LQ and SG chickens. (A) Liver; (B) plasma; (C) cecum.**Figure 2.** Pathway analyses of significantly differential metabolites. (A) Liver. (B) Plasma. (C) Cecum. Bubble size is proportional to the impact of each pathway, and bubble color represents the degree of significance, from the highest (red) to the lowest (yellow).

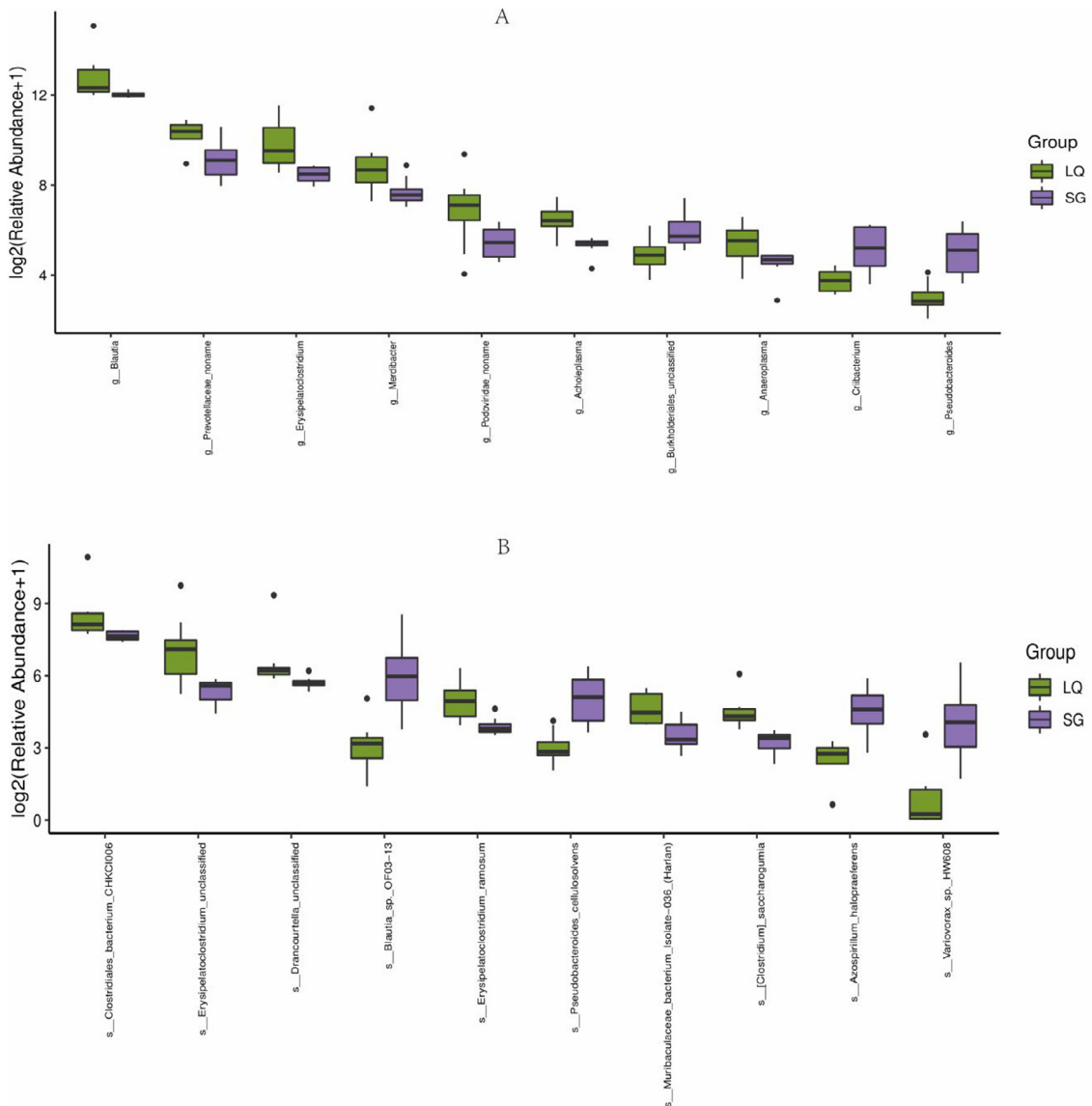
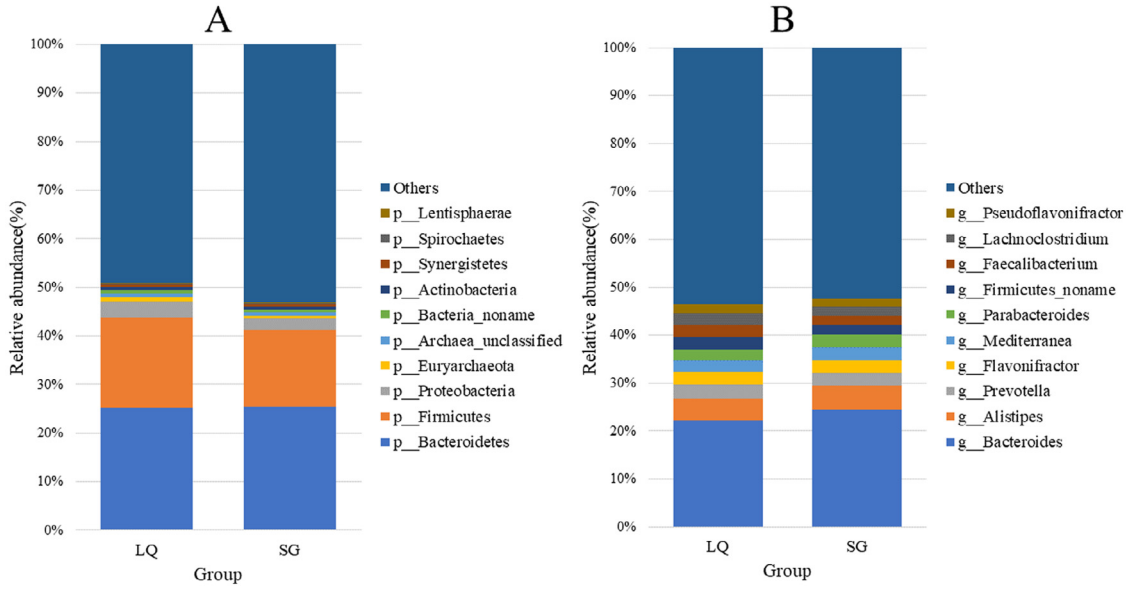


Figure 4. Top 10 different genera (A) and species (B) in LQ and SG chickens.

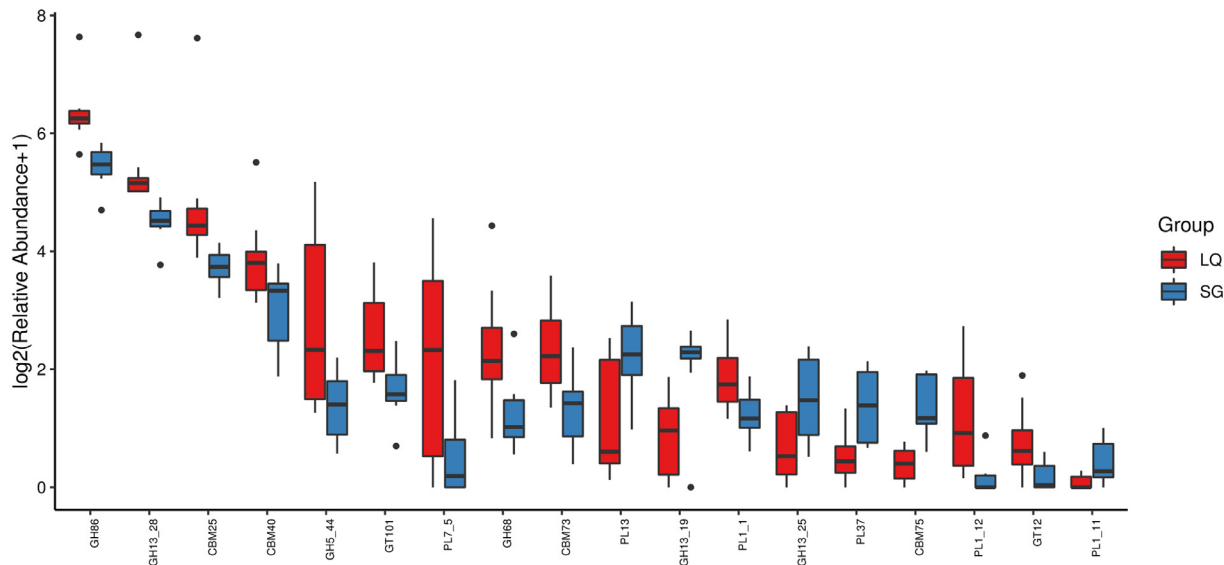


Figure 5. Significant differences in relative abundance of CAZy subsystems between LQ and SG chickens.

chickens. **Figure 6A** shows that the relative higher abundances of Merdibacter, Acholeplasma, Anaeroplasmata, and Prevotellaceae were positively associated with higher concentrations of microbial metabolites in LQ chickens, including mesaconic acid, lysoPG 15:0, and 4,4'-bis(dimethylamino)benzophenone ($P < 0.05$). The relative lower abundances of Burkholderiales, Criibacterium, and Pseudobacteroides were negatively associated with higher concentrations of lysoPG 15:0 and 4,4'-bis(dimethylamino)benzophenone when compared to SG chickens ($P < 0.05$).

Furthermore, the relative higher abundances of six bacterial species in LQ chickens (**Figure 6B**), including Erysipelatoclostridium, *E. ramosum*, and *C. saccharogumia* were positively correlated with the higher concentrations of lysoPG 15:0 and palmitoyl ethanolamide. The relative lower abundances of *Blautia* sp. OF03-13, *P. cellulosolvans*, *A. halopraeferens*, and *Variovorax* sp. HW608 were negatively associated with the higher concentrations of lysoPG 15:0 and palmitoyl ethanolamide and positively associated with the lower concentrations of cis-nerolidol and oxycodone.

DISCUSSION

Fats are the major form of energy storage in chickens and significantly affect meat quality. Chicken breeds possess different growth potentials and fat deposition characteristics. SG chickens, bred in China for 2,000 yr, are a dual-purpose breed. LQ chickens are a broiler species bred by the Poultry Institute of Shandong Academy of Agricultural Sciences. Compared to SG chickens, LQ chickens have a faster growth rate and higher fat deposition capacity. LQ chickens have higher body weight, eviscerated yield, abdominal fat yield, abdominal fat ratio, and higher TG content in breast muscle than SG chickens ($P < 0.05$). Therefore, these chickens can be

utilized as an animal model to study the basic mechanisms of adipogenesis.

In avian species, the liver is the main site of de novo lipogenesis, and hepatic lipid metabolism relates closely to fat deposition (Leveille 1969). Obesity is associated with distinct blood and hepatic lipid profile changes (Kim et al., 2011). We found that several hepatic and blood metabolites associated with lipid metabolic and obesity-related diseases were altered in LQ and SG chickens. Hepatic levels of acylcarnitine 24:6, lysoPE 20:5, and acylcarnitine 26:5 were higher in LQ than in SG chickens. Similarly, plasma levels of acylcarnitine 16:1, palmitoylcarnitine, oleoyl-L-carnitine, stearoyl-L-carnitine, and acylcarnitine 20:1 were significantly higher in LQ. Acylcarnitines comprise molecules where an acyl group is esterified to L-carnitine. Esterification to L-carnitine enables the molecules to cross the mitochondrial membrane (Schooneman et al., 2014; Verbrugghe et al., 2021). Increased plasma acylcarnitine concentrations reflect incomplete beta-oxidation of fatty acids and have been associated with insulin resistance and obesity (Koves et al., 2008). Therefore, the higher acylcarnitine levels in the liver and plasma of LQ chickens than in SG chickens suggest that a large amount of unoxidized fatty acids in LQ chickens is transported through blood circulation to body tissues for deposition, which might explain the higher abdominal fat and muscle TG contents in LQ chickens than SG chickens. Acylcarnitines have been used as biomarkers to diagnose abnormal fatty acid metabolism in humans (Mihalik et al., 2010; Ramos-Roman et al., 2012). Our results confirm that these indexes also apply to chickens, which can be used as markers for chicken fat traits.

Gut microbial diversity affects host factors such as energy and nutrient metabolism. Microbial metabolites such as short-chain fatty acids modulate energy metabolism (Kasubuchi et al., 2015; Overby and Ferguson, 2021). Bacterial fermentation produces short-chain fatty acids, which provide up to 10% of the metabolizable

energy in chickens (Richards et al., 2019). The gastrointestinal microbiota contributes to the regulation of fat deposition, which in poultry seems to be independent of host genetics (Wen et al., 2019). Therefore, the difference in fat deposition between LQ and SG chickens under the same feeding conditions may be attributed to intestinal microbes and their metabolites. As a result, we investigated the microbiome's composition and metabolites in the cecum contents of the 2 chicken breeds, using a combination of high-throughput next-generation sequencing and MS-based metabolomics techniques. We found that the microbiome and metabolome in the cecum were significantly different between LQ and SG chickens. The greatest difference in cecal metabolites was lysophospholipids (**LysoPLs**). Lyso-phosphatidylglycerols (lysoPG 15:0 and lysoPG 16:1) were higher in LQ chickens, while lysophosphatidylcholines (lysoPC 14:0, lysoPC 16:0, lysoPC 16:1, lysoPC 18:3, lysoPC 20:3, lysoPC 20:4, lysoPC 20:5, lysoPC 22:4, lysoPC 22:5, and lysoPC 22:6) and lysophosphatidylethanolamines (lysoPE 16:1, lysoPE 18:2, lysoPE 20:4, and lysoPE 22:6) were higher in SG chickens. LysoPLs are deacylated products of phospholipids with a single fatty acid chain and are produced by phospholipase A (PLA1 and PLA2). LysoPLs include lysoPC, lysoPE, lysophosphatidylinositol (**lysoPI**), lysophosphatidylserine (**lysoPS**), lysoPG, and lysophosphatidic acid (**lysoPA**; Yamamoto et al., 2021). Numerous

studies have suggested that changes in plasma levels of lysoPLs are linked to non-alcoholic fatty liver disease and obesity (Heimerl et al., 2014; Tiwari-Heckler et al., 2018). However, the relationship between lysoPLs produced by microbial metabolism in the gut and host fat metabolism is not thoroughly understood. In our study, there was no significant correlation between lysoPLs produced by microbial metabolism in the gut and lysoPLs content in host plasma and liver. Interestingly, PEA, a key regulator of lipid metabolism, was higher in LQ than in SG chickens. PEA belongs to the endocannabinoid system. The endocannabinoid system has important roles in the gut and adipose tissue physiology, regulating energy balance via multiple mechanisms (Annunziata et al., 2022). Therefore, PEA may regulate intestinal fat absorption, or be absorbed into the bloodstream and modulate systemic lipid metabolism, thus causing the fat deposition differences between the two chicken breeds.

The relative abundance of bacteria in the gut microbiota differed significantly between LQ and SG chickens. The microbiota in LQ chickens is involved in starch and lactose degradation, such as GH86, GH13_28, GH5_44, CBM25, and CBM40, which facilitates the digestion of nutrients and provides the host with more materials for lipid synthesis. We identified the top 10 genera and 10 species with significantly different relative abundance between LQ and SG chickens and analyzed the correlations between metabolites

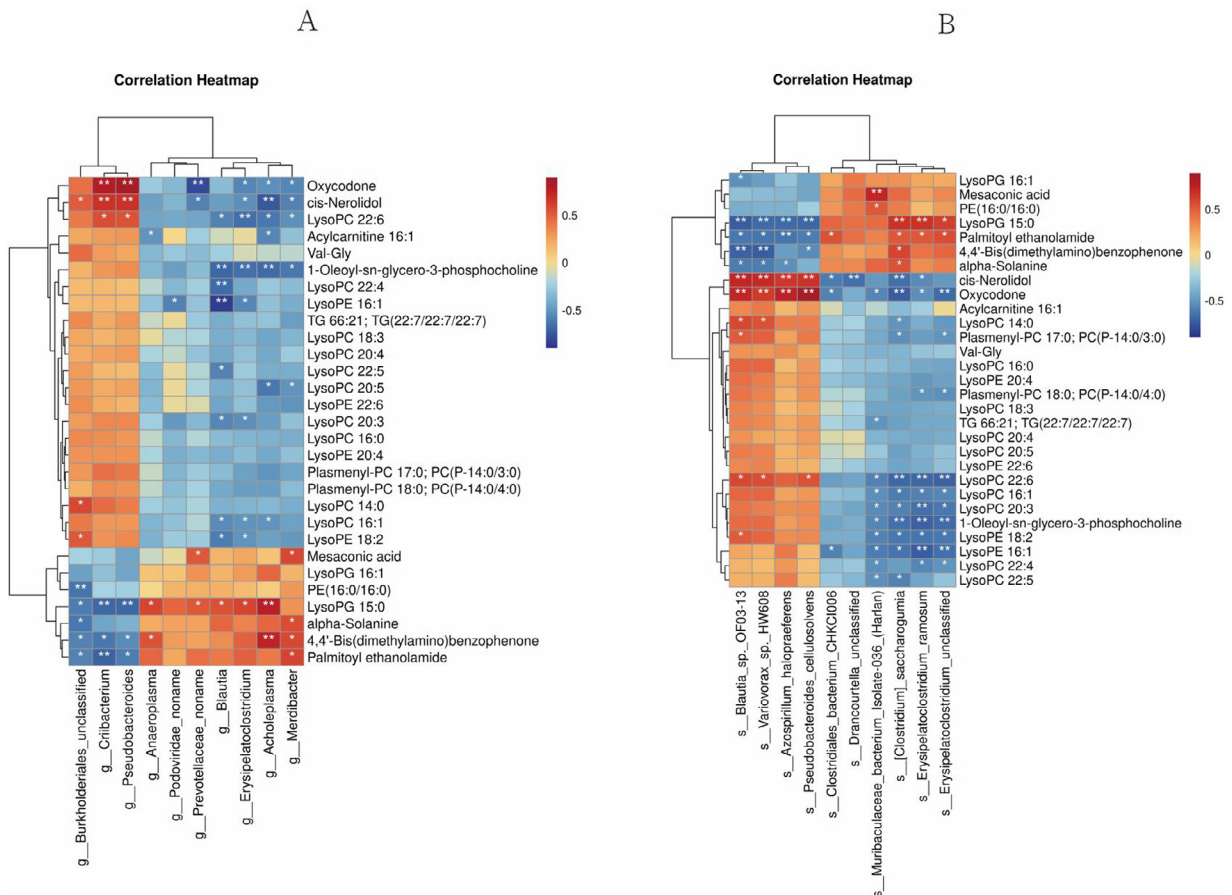


Figure 6. Correlation analysis between microbial communities and their metabolites. (A) Pearson's correlation analysis between cecal genera and metabolites. (B) Pearson's correlation analysis between cecal species and metabolites.

and these microbes. The result showed that *Erysipelatoclostridium* might be important bacteria. *Erysipelatoclostridium* species like *E. ramosum* were abundant in LQ chickens and significantly positively correlated to PEA and lysoPG 15:0. PEA is a key regulatory factor of lipid metabolism, significantly higher in obese people than lean people (Matias et al., 2012). Moreover, *Erysipelatoclostridium* is significantly positively correlated with the abdominal fat percentage in ducks (Zhu et al., 2020). Therefore, the integrated analysis of gut microbiota and metabolites suggests that gut microbes may regulate host lipid deposition through their metabolites.

CONCLUSIONS

Our findings revealed differences in liver and plasma metabolites between chicken breeds with different adipose deposition capacities. Long-chain acylcarnitines might be important markers of adipose deposition differences in chickens. The cecum's microbial communities and metabolome profiles significantly differed between the fatty-type LQ and the lean-type SG chickens. However, the relationship between cecal microbiota and their metabolites and liver and plasma metabolites is not thoroughly understood. Future research should focus on relating tissue metabolite changes to intestinal microbiota and their effects on body fat deposition.

ACKNOWLEDGMENTS

This research was funded by China Agriculture Research System of MOF and MARA (CARS-41). Agricultural Breed Project of Shandong Province (2020LZGC013). Shandong Provincial Natural Science Foundation (ZR2020MC169); Agricultural Breed Project of Shandong Province (2019LZGC019). China Agriculture Research System of MOF and MARA (CARS-40). Agricultural Scientific and Technological Innovation Project of Shandong Academy of Agricultural Sciences (CXGC2022C04). Agricultural Scientific and Technological Innovation Project of Shandong Academy of Agricultural Sciences (CXGC2022D04).

DISCLOSURES

The authors declare that they have no competing interests.

SUPPLEMENTARY MATERIALS

Supplementary material associated with this article can be found in the online version at [doi:10.1016/j.psj.2022.102165](https://doi.org/10.1016/j.psj.2022.102165).

REFERENCES

Annunziata, C., C. Pirozzi, A. Lama, M. Senzacqua, F. Comella, A. Bordin, A. Monnolo, A. Pelagalli, M. C. Ferrante, and

- M. P. Mollica. 2022. Palmitoylethanolamide promotes white-to-beige conversion and metabolic reprogramming of adipocytes: contribution of PPAR- α . *Pharmaceutics* 14:338.
- Baéza, E., M. Jégou, F. Gondret, J. Lalande-Martin, I. Tea, E. Le Bihan-Duval, C. Berri, A. Collin, S. Metayer-Coustard, and I. Louveau. 2015. Pertinent plasma indicators of the ability of chickens to synthesize and store lipids. *J. Anim. Sci.* 93:107–116.
- Braun, E. J., and K. L. Sweazea. 2008. Glucose regulation in birds. *Comp. Biochem. Physiol. B Biochem. Mol. Biol.* 151:1–9.
- Burt, D. W. 2007. Emergence of the chicken as a model organism: implications for agriculture and biology. *Poult. Sci.* 86:1460–1471.
- Cao, M., C. Li, Y. Liu, K. Cai, L. Chen, C. Yuan, Z. Zhao, B. Zhang, R. Hou, and X. Zhou. 2020. Assessing urinary metabolomics in giant pandas using chromatography/mass spectrometry: Pregnancy-related changes in the metabolome. *Front. Endocrinol.* 11:215.
- Dieterle, F., A. Ross, G. Schlotterbeck, and H. Senn. 2006. Probabilistic quotient normalization as robust method to account for dilution of complex biological mixtures. Application in 1H NMR metabonomics. *Anal. Chem.* 78:4281–4290.
- Ghazalpour, A., I. Cespedes, B. J. Bennett, and H. Allayee. 2016. Expanding role of gut microbiota in lipid metabolism. *Curr. Opin. Lipidol.* 27:141.
- Heimerl, S., M. Fischer, A. Baessler, G. Liebisch, A. Sigrüener, S. Wallner, and G. Schmitz. 2014. Alterations of plasma lysophosphatidylcholine species in obesity and weight loss. *PLoS One* 9:e111348.
- Kasubuchi, M., S. Hasegawa, T. Hiramatsu, A. Ichimura, and I. Kimura. 2015. Dietary gut microbial metabolites, short-chain fatty acids, and host metabolic regulation. *Nutrients* 7:2839–2849.
- Kechin, A., U. Boyarskikh, A. Kel, and M. Filipenko. 2017. cut-Primers: a new tool for accurate cutting of primers from reads of targeted next generation sequencing. *J. Comput. Biol.* 24:1138–1143.
- Kim, H.-J., J. H. Kim, S. Noh, H. J. Hur, M. J. Sung, J.-T. Hwang, J. H. Park, H. J. Yang, M.-S. Kim, and D. Y. Kwon. 2011. Metabolomic analysis of livers and serum from high-fat diet induced obese mice. *J. Proteome Res.* 10:722–731.
- Koeth, R. A., Z. Wang, B. S. Levison, J. A. Buffa, E. Org, B. T. Sheehy, E. B. Britt, X. Fu, Y. Wu, and L. Li. 2013. Intestinal microbiota metabolism of L-carnitine, a nutrient in red meat, promotes atherosclerosis. *Nat. Med.* 19:576–585.
- Koves, T. R., J. R. Ussher, R. C. Noland, D. Slentz, M. Mosedale, O. Ilkayeva, J. Bain, R. Stevens, J. R. Dyck, and C. B. Newgard. 2008. Mitochondrial overload and incomplete fatty acid oxidation contribute to skeletal muscle insulin resistance. *Cell Metab.* 7:45–56.
- Kuhl, C., R. Tautenhahn, C. Bottcher, T. R. Larson, and S. Neumann. 2012. CAMERA: an integrated strategy for compound spectra extraction and annotation of liquid chromatography/mass spectrometry data sets. *Anal. Chem.* 84:283–289.
- Langmead, B., and S. L. Salzberg. 2012. Fast gapped-read alignment with Bowtie 2. *Nat. Methods* 9:357–359.
- Langmead, B., C. Wilks, V. Antonescu, and R. Charles. 2019. Scaling read aligners to hundreds of threads on general-purpose processors. *Bioinformatics* 35:421–432.
- Leveille, G. A. 1969. In vitro hepatic lipogenesis in the hen and chick. *Comp. Biochem. Physiol.* 28:431–435.
- Li, W., and A. Godzik. 2006. Cd-hit: a fast program for clustering and comparing large sets of protein or nucleotide sequences. *Bioinformatics* 22:1658–1659.
- Matias, I., B. Gatta-Cherifi, A. Tabarin, S. Clark, T. Leste-Lasserre, G. Marsicano, and P. V. Piazza. 2012. Endocannabinoids measurement in human saliva as potential biomarker of obesity. *PLoS One* 7:e42399.
- Mihalik, S. J., B. H. Goodpaster, D. E. Kelley, D. H. Chace, J. Vockley, F. G. Toledo, and J. P. DeLany. 2010. Increased levels of plasma acylcarnitines in obesity and type 2 diabetes and identification of a marker of glucolipotoxicity. *Obesity* 18:1695–1700.
- Overby, H. B., and J. F. Ferguson. 2021. Gut microbiota-derived short-chain fatty acids facilitate microbiota: host cross talk and modulate obesity and hypertension. *Curr. Hypertens. Rep.* 23:1–10.
- Peña-Saldarriaga, L. M., J. Fernández-López, and J. A. Pérez-Alvarez. 2020. Quality of chicken fat by-products: lipid profile and colour properties. *Foods* 9:1046.

- Peng, Y., H. C. Leung, S.-M. Yiu, and F. Y. Chin. 2012. IDBA-UD: a de novo assembler for single-cell and metagenomic sequencing data with highly uneven depth. *Bioinformatics* 28:1420–1428.
- Pu, Y., J. Pan, Y. Yao, W. Y. Ngan, Y. Yang, M. Li, and O. Habimana. 2021. Ecotoxicological effects of erythromycin on a multispecies biofilm model, revealed by metagenomic and metabolomic approaches. *Environ. Pollut.* 276:116737.
- Ramos-Roman, M. A., L. Sweetman, M. J. Valdez, and E. J. Parks. 2012. Postprandial changes in plasma acylcarnitine concentrations as markers of fatty acid flux in overweight and obesity. *Metabolism* 61:202–212.
- Richards, P., J. Fothergill, M. Bernardeau, and P. Wigley. 2019. Development of the caecal microbiota in three broiler breeds. *Front. Vet. Sci.* 6:201.
- Schooneman, M. G., N. Achterkamp, C. A. Argmann, M. R. Soeters, and S. M. Houten. 2014. Plasma acylcarnitines inadequately reflect tissue acylcarnitine metabolism. *Biochim. Biophys. Acta (BBA)-Mol. Cell Biol. Lipids* 1841:987–994.
- Smith, C. A., E. J. Want, G. O’Maille, R. Abagyan, and G. Siuzdak. 2006. XCMS: processing mass spectrometry data for metabolite profiling using nonlinear peak alignment, matching, and identification. *Anal. Chem.* 78:779–787.
- Stern, C. D. 2005. The chick: a great model system becomes even greater. *Dev. Cell* 8:9–17.
- Tiwari-Heckler, S., H. Gan-Schreier, W. Stremmel, W. Chamulitrat, and A. Pathil. 2018. Circulating phospholipid patterns in NAFLD patients associated with a combination of metabolic risk factors. *Nutrients* 10:649.
- Tůmová, E., and A. Teimouri. 2010. Fat deposition in the broiler chicken: a review. *Sci. Agric. Bohem.* 41:121–128.
- Turnbaugh, P. J., R. E. Ley, M. A. Mahowald, V. Magrini, E. R. Mardis, and J. I. Gordon. 2006. An obesity-associated gut microbiome with increased capacity for energy harvest. *Nature* 444:1027–1031.
- Velagapudi, V. R., R. Hezaveh, C. S. Reigstad, P. Gopalacharyulu, L. Yetukuri, S. Islam, J. Felin, R. Perkins, J. Borén, and M. Orešič. 2010. The gut microbiota modulates host energy and lipid metabolism in mice. *J. Lipid Res.* 51:1101–1112.
- Verbrugghe, A., A. Rankovic, S. Armstrong, A. Santarossa, G. M. Kirby, and M. Bakovic. 2021. Serum lipid, amino acid and acylcarnitine profiles of obese cats supplemented with dietary choline and fed to maintenance energy requirements. *Animals* 11:2196.
- Wen, B., Z. Mei, C. Zeng, and S. Liu. 2017. metaX: a flexible and comprehensive software for processing metabolomics data. *BMC Bioinf.* 18:1–14.
- Wen, C., W. Yan, C. Sun, C. Ji, Q. Zhou, D. Zhang, J. Zheng, and N. Yang. 2019. The gut microbiota is largely independent of host genetics in regulating fat deposition in chickens. *ISME J.* 13:1422–1436.
- Xiang, S., K. Ye, M. Li, J. Ying, H. Wang, J. Han, L. Shi, J. Xiao, Y. Shen, and X. Feng. 2021. Xylitol enhances synthesis of propionate in the colon via cross-feeding of gut microbiota. *Microbiome* 9:1–21.
- Yamamoto, Y., T. Sakurai, Z. Chen, T. Furukawa, S. G. B. Gowda, Y. Wu, K. Nouse, Y. Fujii, Y. Yoshikawa, H. Chiba, and S. P. Hui. 2021. Analysis of serum lysophosphatidylethanolamine levels in patients with non-alcoholic fatty liver disease by liquid chromatography-tandem mass spectrometry. *Anal Bioanal Chem.* 413:245–254.
- Zhu, C., W. Xu, Z. Tao, W. Song, H. Liu, S. Zhang, and H. Li. 2020. Effects of rearing conditions and sex on cecal microbiota in ducks. *Front. Microbiol.* 11:565367.
- Zhu, W., A. Lomsadze, and M. Borodovsky. 2010. Ab initio gene identification in metagenomic sequences. *Nucleic Acids Res.* 38:e132–e132.